High Resolution Shallow Seismic Imaging at an Open Pit Copper Mine

P. Akerberg, D. Dana, A. Levander, C. Zeit and T. Henstock
Center for Computational Geophysics
Geology and Geophysics Department, Rice University, Houston, TX, 77005

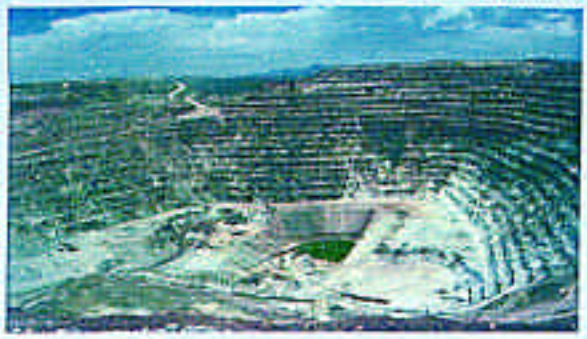

Figure 1
The main pit of the copper mine. The Gila line is along the wall to the right in the picture and the Kem 6 line is along the far wall. The height of each bench is 50 ft.

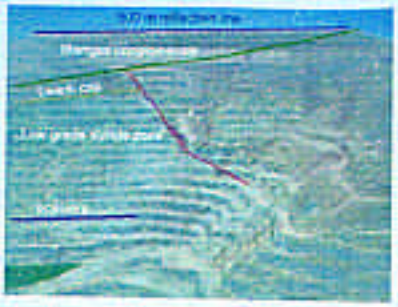

Figure 2
The data for the Gila line consist of a 500 m reflection line and a 500 m transmission line.

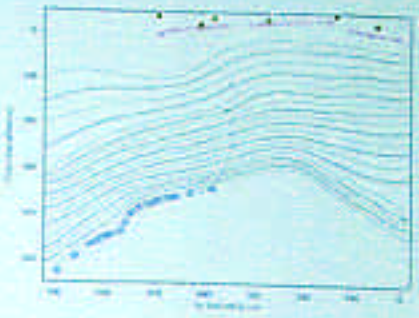

Figure 3
Topography with shot locations for the dynamite data (red) and receiver locations for the transmission line (blue). Boreholes are indicated by green dots.

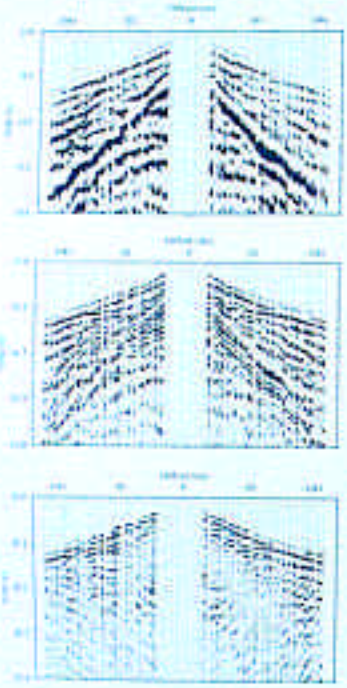

Figure 5
Dynamite CMP supergather before filtering (top), with SCD (middle) and with air-blast attenuation (bottom).

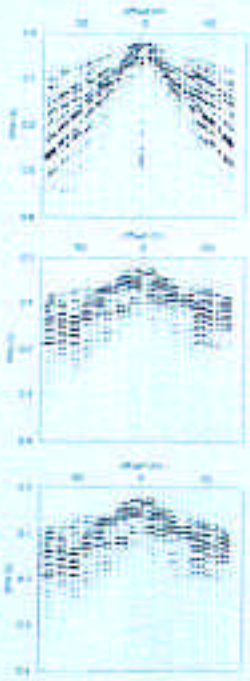

Figure 6
Hammer CMP supergather before filtering (top), with SCD (middle), and after velocity filtering (bottom).

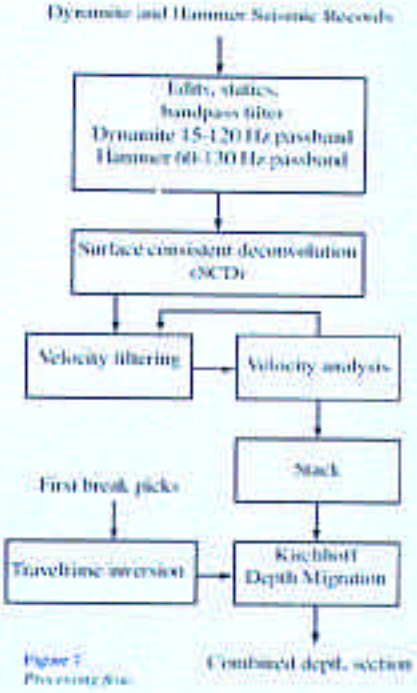

Figure 7
Processing flow.

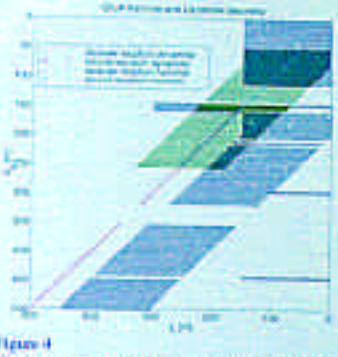

Figure 4
Stacking chart for the hammer and dynamite data.

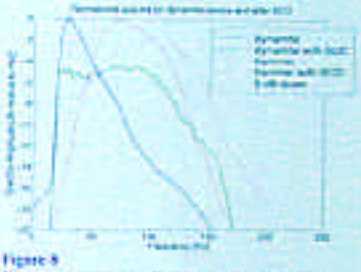

Figure 8
Power spectra for the hammer and dynamite data.

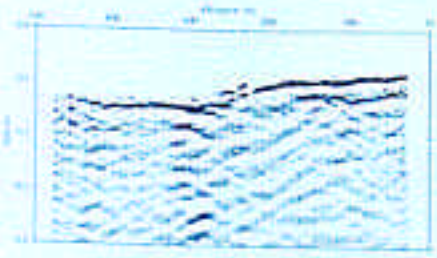

Figure 9
Dynamite data stack. The base of the mine pit corresponds to approximately 300 ms.

Figure 10
Hammer data stack. Ambient noise dominates the stack below 200 ms.

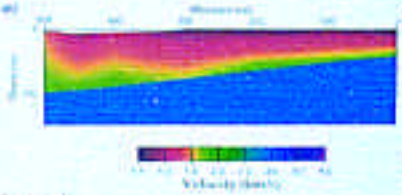

Figure 11
Velocity model obtained from travel time inversion of surface to surface data set. Rays and travel time fits for two example shots used in the travel time inversion (b).

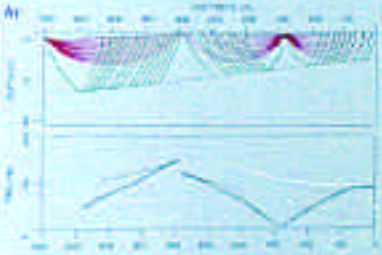

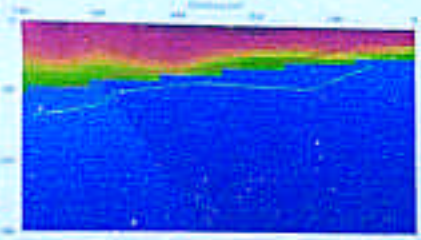

Figure 13
Velocity model from traveltime inversion. See Figure 14 for an explanation of the lines. The velocity model was used for migration.

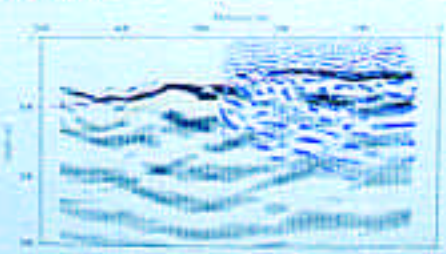

Figure 14
Depth migrated / combined stack. The lines indicate the base of the Mangas compressible and the top of the leach cap.

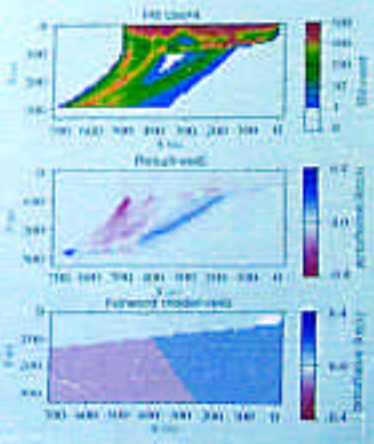

Figure 12
a) "Raw" 1st cover for transmission and surface to surface data through a 2.5 D velocity model.

b) Perturbation obtained by inverting the travel time misfits through a starting model obtained by 2D inversion.

c) Simple forward model based on the inversion result. The model fits the traveltime data to within 5 ms.

Overview

We are developing seismic imaging methods for the near surface which combine conventional reflection and refraction analysis with pre-stack imaging and inversion. This poster shows three projects associated with this research. The first is a seismic field data example from an open pit copper mine (left) which has been processed heavily using conventional methods (through post-stack depth migration). The second is a software environment developed for simulation of wavefields from electromagnetic (radar) (right). The third is 3-D travel time tomography (bottom right).

Introduction

In June 1996, we conducted a high-resolution seismic survey along the rim of an open pit porphyry copper mine in Southwest New Mexico (Figure 1). The survey employed reflection, refraction and transmission profiles in order to image features exposed in the mine walls.

The local geology consists of a sedimentary layer, the Mangas conglomerate, overlying crystalline rock. The crystalline rock includes unaltered country rock and more extensively altered rock. The hydrothermally altered rock can be divided into a zone of mineralization or leach capped over a copper sulphide rich zone that is the primary target for the local mining operation. Underlying it is a barren zone. For this study, targets for imaging include building within the Mangas conglomerate, the unconformity between the sedimentary layer and the crystalline rock, contacts within the crystalline rock, and near surface structural features (Figure 2).

Acquisition and Processing

Dynamite and hammer data were acquired, and processed separately (Figures 3-7). The combination of data from the two source types provides seismic resolution at two slightly different scales (bandwidth of 20-80 Hz for dynamite and 60-120 Hz for hammer) and a validation of individual source results. Following initial data clean up, bandpass filters were used to remove low frequency and 60 Hz noise. Very near surface and mine wall reflections produced a complicated, ringy seismic wavelet. Surface consistent deconvolution operators were calculated for each surface location to compact the pulse, thereby whitening the spectrum (Figure 8). Data from both source types were still dominated by strong groundroll and far more masking the weaker reflections. The coherent noise was removed using velocity filters (Figure 9,10).

Inversion

An initial velocity model was constructed using raytraced 2-D inversion (Figure 11) of the surface to surface travel times. The model was well constrained in the sedimentary layer, but was unable to resolve velocity variations below. By extending the model to 2.5-D (Figure 12) and incorporating travel times from the transmission array we constrained the velocities below the sedimentary layer, and constructed a velocity model for depth migration. Following CMP processing, data from both source types were poststack depth migrated using the velocity model (Figure 13) and combined into a seismic section of the total depth of the mine (Figure 14).

Conclusions

The seismic results correlate with available geologic information and with visible expressions of the formations within the walls of the mine. Specifically, we see: 1) Building within the Mangas conglomerate, 2) the unconformity between the Mangas conglomerate and the underlying crystalline rock, 3) the top of the leach cap, 4) faulting.

The feasibility of simultaneously imaging differences in lithology, contrasts due to mineralogic alterations, as well as structural faulting has implications for directing the

Thanks to
Ralph Stegan at Phelps Dodge Tyrone,
Ed Criley at the USGS, and
the PASSCAL Program of IRIS

References

Zelt, C.A. and Barton, P.J., "3-D Seismic Refraction Tomography: A Comparison of Two Methods Applied to Data from the Faeroe Basin", *Journal of Geophysical Research* 103, 7187-7210, 1998.

Zelt, C.A., and Smith, R.B., "Seismic Traveltime Inversion for 2-D Crustal Velocity Structure", *Geophys. J. Int.*, 108, 16-34, 1992.

A Software Environment for Dispersive Inverse Scattering

William W. Symes
Center for Computational Geophysics
Computational and Applied Mathematics, Rice University, Houston, TX 77005

Simulation Characteristics of Shallow Seismic and GPR:

- Limited aperture / low k scattering
- waves propagate, but are strongly dispersed and attenuated
- typical penetration depths: 20 - 30 wavelengths
- relative sensitive to anelastic / polarization mechanisms as well as to velocity, permittivity, ... variations
- Source/receiver characteristics present formidable modeling, validation problems

Modeling and Inversion Approach

- Finite difference simulation in the time domain, incorporating physical models of propagation, scattering, and attenuation mechanisms: linear viscoelasticity for shallow seismic, dispersive Maxwell for GPR
- with modern high order stencils, FDTD feasible for 3D inversion studies
- Iterative fitting of model parameters P to data D driven by simulation E

$$\min \| E[P] - D \|$$

An Object Oriented Software Environment for Inversion Research:

- abstract time stepping code (C++ class) incorporates canonical framework of time stepping, derivative, and adjoint computations
- time stepping uses stencil operators which wrap standard, optimized F77 implementations - high efficiency, parallelism (300 Mflops on 4 CPU 75 MHz PowerChallenge)
- stencil code for derivatives, adjoints via automatic differentiation
- abstract code for adjoints: Griewank's checkpointing scheme - enabling technology - 1000's of time steps in 3D models in a few Gb, Gflops
- coupled to optimization class library (conjugate gradient, quasi-Newton, ...) through concrete data representation vector classes (SEAY)

Current Status

Basic SEAY vector class, time stepping class with abstract derivatives and adjoints - finished. Several 2/3D simulations under construction.

Three-Dimensional Travel Time Tomography

Colin A. Zelt
Center for Computational Geophysics
Geology & Geophysics Department, Rice University, Houston, TX 77005

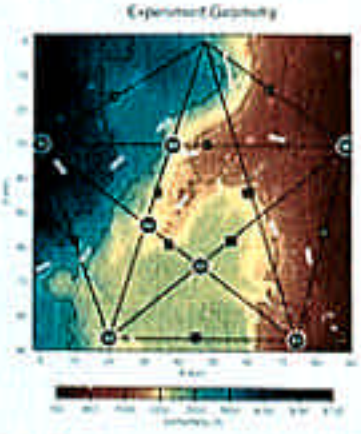

Figure 15
Experiment Geometry for a 3D seismic experiment offshore Chile.

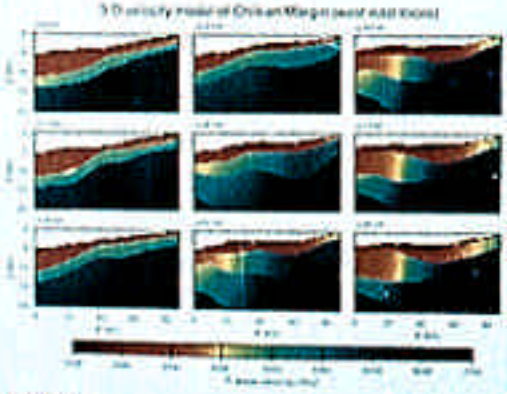

Figure 16
Vertical slices through a 3-D velocity model obtained by tomographic inversion of refracted and reflected times.

Tomographic velocity estimation is used to obtain the long-wavelength 2D or 3D subsurface image for subsequent wavefield processing and imaging techniques that require accurate velocity models. The traveltimes of the pre- and post-critical wavefield are used in a fully 3D tomographic technique to estimate the smooth velocity model, making no assumptions or approximations other than that of the infinite-frequency eikonal equation. The method of traveltime calculation is computationally fast in 3D, handles large velocity contrasts, and computes both reflection and refraction times. Traveltimes are inverted for velocity and interface structure in a combined, simultaneous reflection and refraction tomographic method. Regularization is included in the inversion to provide smooth, layered models, a desirable feature for later processing steps, and to allow incorporation of prior information, such as well velocities, boundaries, or faults.

Tomographic velocity estimation requires the analysis of a large number of data gathers for arrival picking guided by traveltime reciprocity and the traveltimes predicted by progressively more complex models as more data is included in the inversion. Reflections and refractions from key horizons are picked from pre-stack data; reflection times from unmigrated stacked data may also be used in the inversion.

A real data example of a preliminary 3-D model obtained by simultaneous inversion of refracted and reflected traveltimes from several layers is shown in Figure 16 as a series of parallel, vertical slices through the model. The experiment geometry for this marine survey is shown in Figure 15; the seven ocean bottom receivers (large black dots) and ten shot lines are labeled.

Although this is a crustal-scale example with a relatively small data volume, the layering and relative 3-D heterogeneity, both laterally and vertically, is not dissimilar from what might be expected in the shallow environment.

Contact Information :

alan@geophysics.rice.edu
czelt@geophysics.rice.edu
symes@caam.rice.edu

http://terra.rice.edu

Center for Computational Geophysics, MS-126
Rice University
6100 Main Street
Houston, TX 77005